



## Audio Engineering Society Italian Section

Seminar – 20 september 2003 – Milano (ITALY)  
“LOUDSPEAKERS AND NONLINEARITIES”

*This paper has been reproduced from the authors' advance manuscript. The AES – Italian Section takes no responsibility for the contents. Reproduction of this paper, of any portion thereof, is not permitted without direct permission from the authors and the AES – Italian Section. Contacts: [www.aesitalia.org](http://www.aesitalia.org) and [info@aesitalia.org](mailto:info@aesitalia.org).*

---

## A Novel Synthesis Approach to Loudspeaker Design

M. Navarri, E. Bellati, F. Tordini, R. Toppi  
FAITAL SpA – San Donato Milanese

## 1. INTRODUCTION

Fundamental works on loudspeaker modeling by R.Small and N.Thiele [1-3] established a successful framework to describe loudspeaker behavior at low frequencies, using lumped elements mechanical and electro-acoustical equivalent circuits (fig.1,2). In this framework the most fundamental parameters are assumed to be constant, i.e. the driving signal is low enough to justify the small excursion assumption. It is common practice to use the T.S. parameters when designing loudspeaker cabinets, acoustical transmission lines, or horn loaded systems where, once again, the linear model is applied.

Of course, as “small signals” have almost no real-world counterparts, it’s easy to verify the limits of the linear model assumption. In fact, a functional description for the parameters is needed when the moving mass exhibit large excursions and the T.S. coefficients show a strong dependence on the moving mass position. Low frequency distortion and “power compression” phenomena reveal the presence of harmonics other than the fundamental one and explicitly show how the linear paradigm fails in the large signal case.

Unfortunately the quality of reproduction at low frequencies is not always well predicted by traditional measuring techniques, i.e. high distortion figures do not always correspond to poor sounding loudspeakers, and recently some researchers have worked to establish a correlation between objective and subjective (listening tests) quality measures.

Lately, the automotive industry also focused its attention onto this research field to provide a higher quality in-car listening environment to their customers.

The desire to improve loudspeaker models leads to the development of new techniques that try to embed the nonlinear behavior into the model; the works of D.Clark [7] and W.Klippel [4-5] are

significant examples of this tendency, and they all rely on measurements of assembled, fully working loudspeakers.

Moreover, better knowledge of transducer models together with an extremely competitive market, boosted the amount and complexity of the specifications that loudspeaker manufacturers have to address when designing a new component or system. Of course, improved modeling techniques and deeper knowledge of components are necessary but not sufficient as time-to-market has to be continuously reduced. Therefore, minimizing the time needed to produce prototypes fulfilling all the specifications requested by the customer becomes a key point. The next step is the development of adequate software tools that let the designer chose between different component setups to achieve the best results without actually assembling the prototype and thus avoiding the traditional and time consuming trial-and-error strategy.

This work addressed the development of an original methodology that allows the loudspeaker designer to assemble virtual prototypes and then measure their characteristics at low frequencies (i.e. the “piston range” of T&S). Next section presents the fundamental idea behind this work, while section two gives the details of the mathematical model used. Section three discusses the virtual prototype assembly, and section four describes some aspects of the components. Section five is dedicated to the loudspeaker and measurement setup, and to the analysis and comparison of virtual and experimental measurements; the auralization of the model has been introduced. Conclusion remarks and open problems are discussed in the last section.

## 2. THE NOVEL STRATEGY

The development of a new loudspeaker begins with a list of specifications required by the customer: the designer’s goal is to translate them into design constraints to define a (possibly small) set of component candidates. Various configurations are

then assembled and the resulting prototypes are then measured to help decide which is the optimum configuration.

This procedure is traditionally a trial-and-error process guided by experience and, even if conceptually simple, it is clearly the most expensive and time-consuming way to get to the point (usually more than one prototype is assembled for each setup, and everything is done by hand; as a side effect, documentation grows exponentially with the number of possible configurations).

Some questions arise quite naturally: is it possible to work on virtual prototypes? Can we perform all kinds of measures on these “loudspeakers” to verify whether they satisfy or not customer specifications? Can we rely on this virtual environment to choose the best component setup?

### 3. THE MATHEMATICAL MODEL

Let’s take the T.S. model as a reference. All its components can be represented as constant parameters under the small signal hypothesis, meaning that the moving mass oscillates in the neighborhood of an equilibrium point. When this assumption no longer holds (if we drive the loudspeaker with higher voltages, for example), the parameters of the model become functions of the moving mass position [5,7-8]. In the following, the electrical resistance ( $R_e$ ) of the voice coil and the mechanical losses ( $R_{ms}$ ) are still treated as constants, while compliance values of the suspension components (spider and membrane), driving force, and inductance are described by non-linear models.

#### 3.1. The Algorithm

All calculations have been performed using MathCAD<sup>1</sup>. This environment allows great flexibility when defining driving signals or new algorithms. In fact,

the simulation shell has been thought as an acquisition card where an analog input signal is fed to the model; then, the “state space” vector is sampled at defined time values and the output is stored in memory. At this point we have all the information we need regarding the “loudspeaker”: it is only a matter of extracting the features we are interested in

Before going into details, the definition of the parameters used by the model is given..

- $C_m(x)$ : resulting compliance of spider and cone edge
- $M_{ms}$  : total mass (including air load) of the moving parts
- $R_{ms}$ : mechanical resistance of total-driver losses
- $Bl(x)$ : force factor
- $R_e$ : electrical resistance of the voice coil
- $L_e(x)$ : electric inductance of the voice coil
- $L_{fe}(x)$ : voice coil inductance due to electromagnetic force

The differential functions governing the process are well known:

$$e(t) := R_e i(t) + \frac{d}{dt}[L_e(x)i(t)] + Bl(x)\frac{d}{dt}[x(t)]$$

$$Bl(x)i(t) := M_{ms} \frac{d^2}{dt^2}[x(t)] + R_{ms} \frac{d}{dt}[x(t)] + \frac{x(t)}{C_{ms}(x)} + L_{fe}(x) \frac{i(t)^2}{2}$$
(1)

These equations can be simplified as discussed in the next section, leading to:

$$e(t) := R_e i(t) + L_e \frac{d}{dt}i(t) + Bl(x)\frac{d}{dt}[x(t)]$$

$$Bl(x)i(t) := M_{ms} \frac{d^2}{dt^2}[x(t)] + R_{ms} \frac{d}{dt}[x(t)] + \frac{x(t)}{C_{ms}(x)}$$
(2)

The system can then be rewritten in a more convenient way using its state space representation,

$$\frac{d}{dt}X(t) := A(x) \cdot X(x) + B \cdot e(t) ,$$
(3)

with:

<sup>1</sup> MathCAD is a trademark of MathSoft Inc.

$$\begin{aligned}
 X(t) &:= \begin{pmatrix} x(t) \\ v(t) \\ i(t) \end{pmatrix}, \quad B := \begin{pmatrix} 0 \\ 0 \\ \frac{1}{L_e} \end{pmatrix} \\
 A(x) &:= \begin{pmatrix} 0 & 1 & 0 \\ -1 & \frac{-R_{ms}}{M_{ms}} & \frac{Bl(x)}{M_{ms}} \\ M_{ms} C_{ms}(x) & \frac{-Bl(x)}{L_e} & \frac{-R_e}{L_e} \end{pmatrix}
 \end{aligned} \tag{4}$$

and where  $e(t)$  represents the loudspeaker driving signal. Solving the differential equation using classical numerical algorithms, it is possible to calculate the evolution in time of voice coil displacement and velocity, together with the current running in it.

Once the model is defined it is easy to feed the input signal  $e(t)$  which is most appropriate to the test that the designer wishes to perform on the loudspeaker. In fact, all kinds of measures can be easily implemented. If we consider the harmonic analysis, for example, sound pressure, traditional and Blat distortion [6,9] can be evaluated. All frequency dependent measures are easily carried out feeding the model with a sinusoidal input  $e(t) := e_0 \sin(2\pi f_0 t)$ , where  $f_0$  values can follow a predetermined law (R80 spacing, for example).

### 3.2. Simplifications of the model

When we started this work we had clear in mind that a model is just one possible representation of a physical process, not the process itself. Therefore, the goal was the development of a tool that could provide useful information regarding loudspeaker's performance, and then act on the critical components to obtain the closest approximation to the desired response. The difficulties that arose from for the definition of the models of some quantities triggered further investigations, as mentioned in the last section.

However, the simplifications introduced here are assumed not to impair the validity of the model. Once again, one

goal of this work is to define a tool that can speed up the design process helping the engineer in taking critical decisions about component specifications. This means that the virtual assembly of the loudspeaker (component characterization) must be fast and practical: the expected output is a qualitative measure of the loudspeaker's performance.

The model must then be able to highlight the problems arising from a certain component setup. Of course, divergence between predicted and real measurements must be carefully analyzed to continuously improve the model.

First simplification concerns the value of the inductances  $Le(x)$  and  $Lef(x)$ : a dynamical FEM analysis is needed to obtain a solution to the problem as described by equations in (1). In fact inductance value varies with the position of voice coil in the air-gap: the calculation of a value for each position of the coil is a lengthy procedure that we decided to avoid by considering constant values. A slight underestimate of excursion figures at low frequencies is the trade-off between model accuracy and computational load.

Next release of the software will instead include thermal aspects: here we assume a constant temperature (and hence resistance  $R_e$ ) for the coil.

Moreover, hysteresis and “creep factor” modeling [10] of the suspension have not being addressed in this paper as it is the object of current research, together with the contribution to the overall compliance due to the compression of the air under the dust-cap.

## 4. THE VIRTUAL LOUSPEAKER ASSEMBLY

Next step is defining the concepts of “virtual assembly” and “virtual measurement”. At low frequencies all loudspeaker components have well defined mechanical functions within the system, and their behavior (whether electrical or mechanical) can be easily measured. The spider, for example, can be modeled as a spring and its functional

representation can be the classical force/displacement curve. While in the linear model this function is assumed to be constant, it is well known that the actual curve is indeed non-linear. Therefore we introduced the compliance curve into the model.

Exploring the behavior of each component and using the functional relations among them, one can actually assemble a virtual loudspeaker, and hence perform any measurement over it.

#### 4.1. Advantages and drawbacks of the method

The first main advantage lies in the fact that non-linear behavior of the components is not represented by mathematical functions as in many other approaches (exponential and quadratic functions are among the most used approximations [6-7]). This might sound rather inelegant from the model point of view, but, due to the complexities and unpredictability of non-linear behaviors of real components, function approximation strategies tend to fail. This point is underlined if we leave the neighborhood of the moving mass equilibrium point (i.e. for higher driving voltages). This would lead to a great effort in developing more intelligent (and complex) prediction algorithms that guarantee a good fit with the data in the large signal case.

We instead decided to rely only on real measured data. In fact, population characteristics are rather uneven in the case of many components; moreover, the need to improve our knowledge of material properties suggests the need to perform an in-deep experimental study for each component type. These two factors, together with the variety of components that should be characterized, naturally lead to the use of real measured data instead of functional approximation.

This approach has a second advantage. Once a component (with its own geometry and material properties) is characterized, it becomes a part of a library. When defining a new project is then sufficient to specify the geometrical constraints for the components, to gather all the possible

setups. Choosing the best design is then an easy and quick job.

Moreover, once we have a selection of model candidates, it is rather easy to calculate the auralization in each case – the musical signal is just another  $e(t)$  to be used as input to our model. It is sufficient to apply to the musical signal of a scale factor related to the desired driving power to listen to the effects of the non-linearity of the loudspeaker we have “in hand”.

Of course, this software environment is also a powerful design tool for new components as it can be used in a synthesis-fashion manner to specify the ideal behavior (response curve) for each component, shifting the trial-and-error approach from the real world to this virtual one (with obvious advantages in terms of time and resources).

So far, the major drawback of our approach lies in the difficulty of modeling certain parameters with a dynamical behavior as  $Lx(x)$  and  $Rms$ . In fact, the measuring techniques we used to characterize most components are either static or semi-static, and removing this restriction is a matter of current research.

## 5. COMPONENT CHARACTERIZATION

This section is devoted to the description of the parameters used during the simulations.

### 5.1. The voice coil

The voice coil travels in the air-gap driven by the force resulting from the balance of the surrounding magnetic field and the one due to the current running in it. In the “piston range” the moving mass follows the same behavior. Ohm’s Law relates voice coil resistance, length and section of the coil conductor.

Given the diameter of the voice coil and its expected resistance, the height of the coil is easily calculated. Turning to the model, the relevant parameters are two: conductor length and coil height. The first one is used in conjunction with the force

factor to calculate the “ $Bxl$ ” term, while the coil height is important in defining the linear excursion range of the voice coil in the air-gap, as detailed in section 4.2.

## 5.2. The magnetic motor

The characterization of this component, together with the analysis of the voice coil model, gives all the information regarding the force driving the moving mass of the loudspeaker and the inductance value.

We used a well-assessed and carefully verified FEM technique to calculate the magnetic flux density in the air-gap. This tool provides good design indications to the engineer regarding the trade-offs between mechanical (dimensions and weight) constraints over the magnetic circuit and its performance.

Moreover, the FEM can easily calculate the field values in each point (or region) of the space. Particularly interesting are the values of the flux density in the air gap, especially along the voice coil trajectory in the assembled loudspeaker.

Of course, each section of the coil experiences a different value of flux density, but a good approximation is represented by the average flux given by the integral calculated along the coil. This average has to be calculated for all possible positions of the voice coil within the air-gap: from the bottoming position to its symmetrical one with respect to the correct on-field position.

The result of this procedure is shown in fig.4, where the evolution of  $B$  with respect to the moving mass position is given. The first useful information is given by the analysis of the shape of the curve. The width of the bell, its symmetry and position of maximum value, the max-excursion possible for a given height of the voice coil, are some of the most important points that help in optimizing the magnetic circuit with respect to the required specifications.

From here, we can decide the values for the voice coil height, the material and the geometry of the magnetic circuit, and the on-field position of the voice coil to

achieve the desired flux density values along the trajectory of interest.

## 5.3. The spider

The spider is one of the “springs” in the mechanical model of the loudspeaker, and can be easily modeled by a displacement/force curve related to the movement of its neck. The actual technique uses a known mass applied to the spider’s neck, and the measurement of the relative displacement. Of course this method only gives information over one point of the compliance curve of the spider and was inadequate to our purposes.

As with the magnetic circuit we started with the FEM approach, but the results are still not satisfactory mainly because of the difficulties in characterizing the mechanical properties of the materials involved.

For this reason we decided to continue the development of the FEM approach but not to include it in this software release. Instead, we turned to a semi-static measurement system which can easily provide the compliance curves of the component under realistic working conditions: the spider is glued to a basket-like clamp and the neck to a plug acting as the voice coil. The measurement system simply applies a known displacement and measures the force opposed by the spider at each step. Pre-cycles are performed on each spider to avoid problems due to first-curve measurements, while the max-displacement value was set slightly higher than the assumed typical excursion for the loudspeaker under test. In fact, if higher excursions are needed during the measurements on the virtual prototype, a mathematical extension of the tails of the compliance curve is performed with a simple fitting algorithm.

The only other data needed by the model is then the maximum mechanical excursion allowed (a value that can only be deduced from an ensemble-study of the particular loudspeaker configuration).

From measurements carried out on a number of spiders and from the analysis of the expected performance of the

loudspeaker, the critical role played by this component clearly emerges. In fact, spiders which are identical by design can show quite different behavior and this can cause deviations of the performance figures up to 50% (this is also an important factor to consider when analyzing the divergence of virtual and real-world measures experienced with some test-loudspeakers).

As usual, this synthesis oriented design process also allows a deeper comprehension of component interactions and criticalities, especially when large excursion are considered.

#### 5.4. The membrane

Presently, the only technique known by the authors and described in literature providing a characterization of the membrane relies on the measurement of the resonance frequency of the cone [11]. As for the case of the spider we frozen the FEM approach to follow the semi-static measurement strategy. The membrane is composed of a cone (simply a constant when considering the moving mass weight) and its edge, which is the second “spring” of the mechanical model sketched in Fig.1. The compliance of the membrane is then measured in much the same way used for the spider.

The compliance curve measured after some pre-cycles, the value of the maximum allowed excursion, and the contribution to the overall moving mass, are then fed into the model.

#### 5.5. The suspension: spider and membrane

As expected the spider and the cone edge behave as two springs tied to the same points (Fig.1), and the resulting compliance is given by the combination of the two, namely  $C_s(x)$  and  $C_e(x)$ :

$$C_{ms}(x) := \left( \frac{1}{C_s(x)} + \frac{1}{C_e(x)} \right)^{-1} \quad (5)$$

#### 5.6. The dust cap

For the frequency range of interest, the dust cap is considered only a passive component of the overall moving mass. Its weight is always available from the respective drawings.

#### 5.7. Other masses

Other contributions to the overall moving mass weight are given by the air volume moved by the cone (a function of its active surface), and by the mass of other elements such as glues, lead wires, etc.

### 6. THE MEASURES

Quite a number of measures trying to provide a characterization of the loudspeaker response exist. The measurement techniques can be either direct (the measure of a given physical quantity) or indirect (algorithms extracting other performance figures from the value stemming from direct measure). However, the state space description allows the designer to calculate any performance figure required by the customer. Here we choose to concentrate on various aspects of the moving mass excursion, but it is obviously only a sample of the information that can be extracted from the virtual loudspeaker performance.

#### 6.1. Definition of the loudspeaker under test

Because of the number of variables involved in the setup of a loudspeaker, we decided to concentrate on the spider to highlight the possible errors in the model. The spiders set was chosen to provide different nominal compliance values and also considering different manufacturers for each model.

The membrane chosen showed a clear asymmetric behavior that affected the linearity of the spider once the overall suspension compliance is considered. Fig.5 reports the compliance curves of spider, cone edge and their combination, as calculated using equation (5).

The voice coil height was 3.7mm, slightly shorter than the upper plate: small displacement values are then sufficient to cause dramatic variations in the average flux density experienced by the coil. The first set of test samples using this configuration is detailed in Table 1.

To cross-validate the results we also chose one particular configuration among the ones in Table 1, and then varied other parameters as voice coil height and on-field position (Table 2). This way we could verify the robustness of the model in respect to a number of parameter variations.

## 6.2. The instruments

Excursion measurements were performed using a laser displacement meter: this way we could immediately compare experimental results with the expected ones provided by the model.

The loudspeaker is adequately fixed to a vertical plane to minimize gravity effect on the moving mass, and it operates in free field conditions. Measurement setup and connection scheme is sketched in fig.3. The external audio amplifier supplies the required power to drive the loudspeaker with minimal distortion levels.

The audio analyzer generates a sinusoidal sweep (following the R40 standard) in the [20-200Hz] range, where the excursion values are more relevant.

The laser reads the position of the center of the dust-cap and, considering the frequency range, this exactly represents the position of the entire moving mass. The reading of the displacement meter is sampled only after the end of the attack transients of the loudspeaker, to avoid aliasing problems.

A full harmonic analysis can then be performed using the sampled signal; in particular, we focused our attention on the first three harmonics using selective tracking filters.

## 6.3. Results

Comparisons of simulation and real measurements of moving mass position

are presented in figs.6-11. In particular offset (the dynamical equilibrium position of the moving mass), fundamental, second, and third harmonic values are reported. The correspondence of simulated to experimental values can be regarded as a fairly good test to evaluate the model accuracy and reliability.

All sample loudspeakers of Table 1 were measured showing similar results to the corresponding simulations. Due to space limitations, here we only reported the most significant examples.

Fig. 6 reports the measures over sample #5: simulated and the experimental curves show a good matching with a slight difference on offset values.

For driving voltages as low as 4V the results provided by the model are even closer to the experimental ones (fig.7) for all configurations. The next step was moving onto higher driving voltages (6V) to test the model reliability for larger excursion values.

As already said in section 4, the great influence of spider compliance values dispersion over the overall response clearly stem from the measurements [10], and is summarized in figs. 6 and 8. For these loudspeakers, we used exactly the same setup – spider model, manufacturer, and production lot – but the matching of the simulated results with the experimental ones strongly depends on the choice of the spider compliance curve using for the simulation. Even if spider #1 and #2 are nominally identical, the difference in their compliance figures is not negligible and, clearly, the one used to assemble Sample #5 is much more similar to spider #1 than to spider#2. In fact, assuming a lower compliance results in lowering all the curves (fig. 8). On the other hand, as the shape of the two spider curves is the same, the shapes of the expected response curves are still representative for the chosen loudspeaker sample.

Figs. 9 to 11 summarize the results obtained by varying parameters other than the spider. In particular, we focused on the magnetic circuit characteristics. Fig. 9 describes the results for Sample #3: with

respect of Sample #5 we observe a much higher offset value, which was well predicted by the model. The same loudspeaker configuration was assembled using a different on-field position for the voice coil (1mm closer to the lower plate): results are presented in Fig.10. In this case, there is a difference between simulated and experimental curves for the first harmonic (max. error 0.5mm) at very low frequencies (error for the third harmonic is lower than 0.25mm). The reason for this behavior has to be found in the dispersion of the spider characteristics (once again), since it was sufficient to scale slightly the compliance curve to obtain a perfect fit.

The last example (fig.11) considers a loudspeaker with a larger voice coil height (6mm instead of 3.7mm). Also in this case the true compliance curve of the spider must have been slightly higher than the one used for the simulation as all curves are under-estimated by the model.

As a general rule, the model shows a good accuracy and the differences, if any, are found in the lower part of the considered frequency range. Apart from the dispersion on the spider compliance value, this misbehavior also is a measure of the approximation coming from the exclusion of thermal aspects from the model. In fact, the measuring system accepts the measure only once the attack transient is concluded; during this short and yet finite interval, high currents run in the coil, influencing its temperature and, hence, its resistance. This phenomenon is much more evident the higher the driving voltage is.

Eventually, the finite accuracy of the laser displacement meter has to be considered when analyzing the results.

#### **6.4. AURALIZATION OF THE MODEL**

Among the developments foreseen for this tool presented in a previous work [12], there is the capability to give an even more “realistic” feedback to the designer with the possibility to drive the virtual loudspeaker with a generic signal. The input signal can be a “.wav” file which is

first normalized to its r.m.s value, so that it can be representative of the nominal power we want to drive the loudspeaker (this simulates exactly the reading from the probes of a r.m.s. voltmeter across the loudspeaker terminals). Driving the model with the normalized signal we can easily calculate the pressure level produced by the loudspeaker.

This simple sequence of operations gives infinite degrees of freedom in terms of simulation possibilities. For example, the input file can be a test signal suited for other types of distortion or the basis for new tests (i.e. complex intermodulation, simple and multiple-burst stimuli, modulated noise, ...).

Of particular interest can be the evaluation of the audibility of the distortions due to the loudspeaker's components, taken individually: using a music program or speech as input signal we can hear the potential effects of the non-linearities, and have an additional subjective parameter for performance judgement.

## **7. CONCLUSIONS**

This work introduced an innovative synthesis-oriented loudspeaker design strategy focusing on low frequency range performances. Most importantly, the results showed that the model adopted is indeed accurate in predicting the behavior of the moving mass, giving precise indications over important features as distortion figures and bias.

Simplifications introduced in section 2 are then justified by the matching of simulated and experimental results.

The result is a time-saving software design tool that allows the optimization of existing components (constituting a virtual library) and the specifications of new ones to match customer requests. Moreover, it can also be regarded as a full-featured virtual test bench for loudspeaker prototypes.

Excellent results have already been achieved using this technique, which proves the reliability of the method.

The tool also features the capability of auralize any input signal which leads to the possibility to perform virtually any kind of test. Moreover, the auralization is an effective subjective technique to evaluate the high-power performance of the loudspeaker.

Nevertheless, spider modeling still needs further investigation because of the critical role it plays in the overall performance, and due to the high variability of its characteristics. Lastly, the upgrade of the model to include other phenomena such as the thermal effect, is the object of current research

Since the previous work [12] the model has been testing on various projects with excellent results. The accuracy of the predictions have allowed us to take correct decisions during the development of several new loudspeakers.

Nominal Compliance / Supplier	0.8mm/N	1.0mm/N	1.6mm/N
A	-	-	Sample 7
B	-	Sample 3	Sample 8
C	Sample 1	Sample 4	-
D	-	-	Sample 9
E	-	Sample 5	Sample 10
F	Sample 2	Sample 6	Sample 11

Table 1. Configuration setups used for sample assembly. Each sample differs from the other for the spider used.(compliance value and manufacturer)

Sample No.	Variable
# 12	As sample #03 but with different voice coil on-field position (-1.0mm)
# 13	As sample #03 but with different voice coil height (+2mm)

Table 2: Variations over Tab.1 configurations. Chosen a certain spider, these changes allow the cross-validation of the model in respect to magnetic circuit variations.

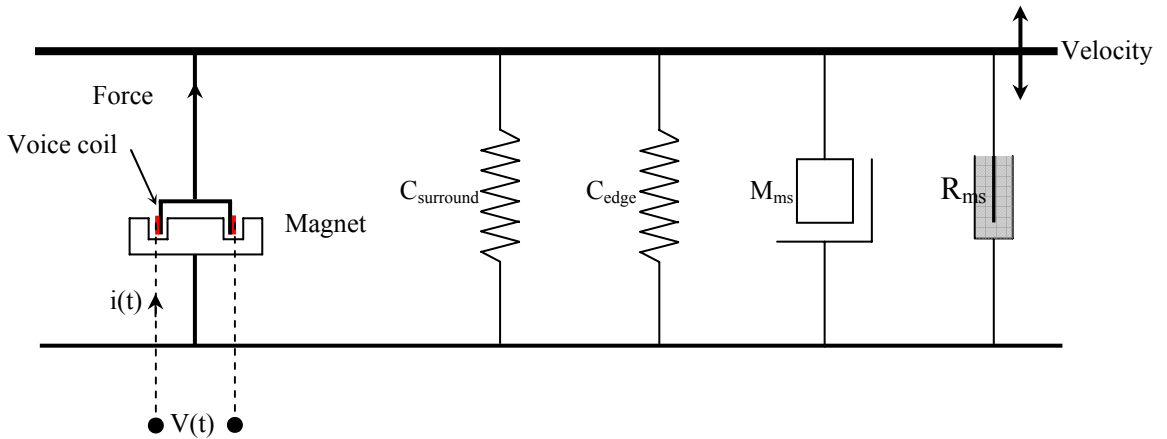


Fig. 1 (Low frequency) mechanical model of a loudspeaker

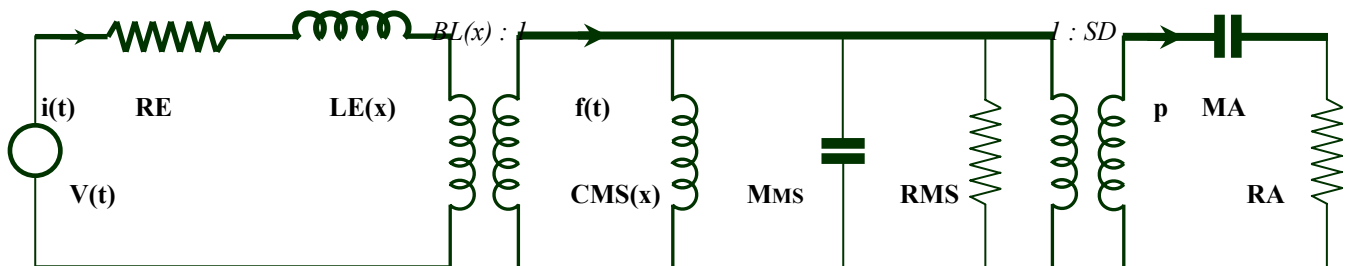


Fig. 2: (low frequency) equivalent electrical circuit of a loudspeaker.

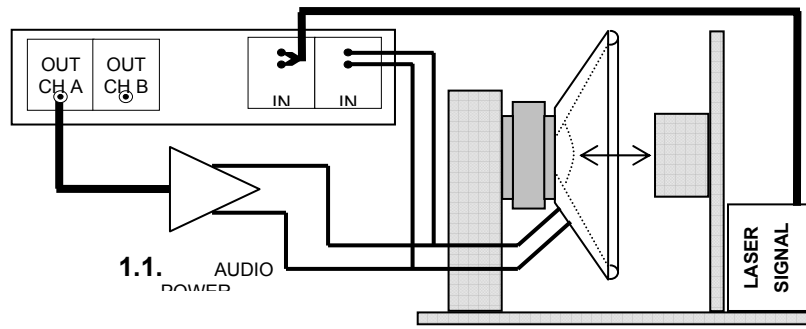


Fig. 3: Excursion measures connection scheme and setup.

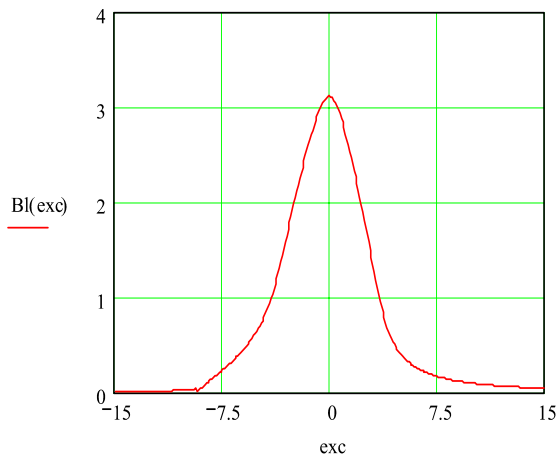


Fig. 4: “ $Bl$ ” curve of the magnetic circuit as a function of voice coil position in the air gap.

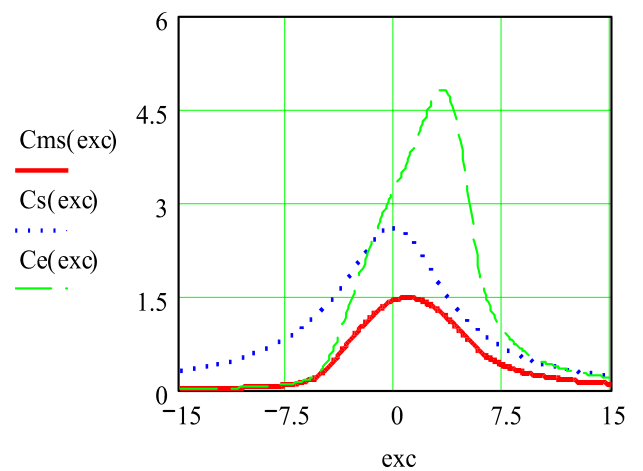


Fig. 5: compliance curve of components which exhibit elastic behavior. (—) Resultant compliance curve; (...) Measured spider compliance curve; (---) measured cone-edge compliance curve

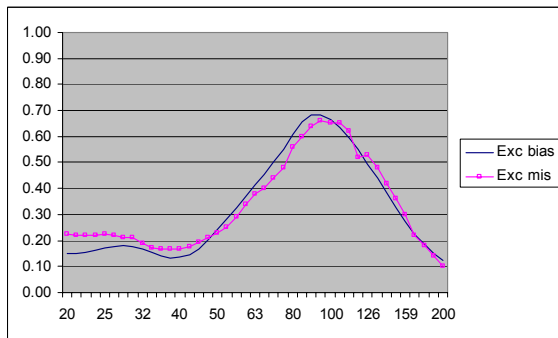


Fig. 6.1. Sample #05: bias curve associated to the moving mass equilibrium point. Loudspeaker driven @6V.(\*)

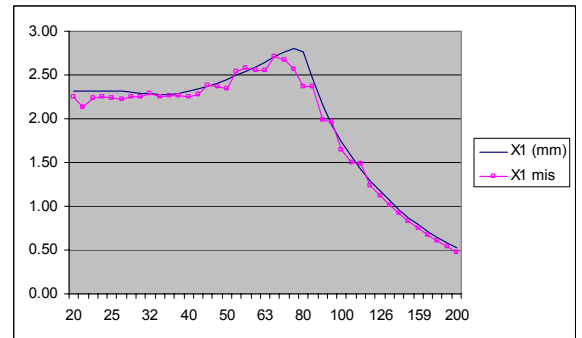


Fig. 6.2. Sample #05: 1st harmonic curve (fundamental) of moving mass excursion. Loudspeaker driven @ 6V. (\*)

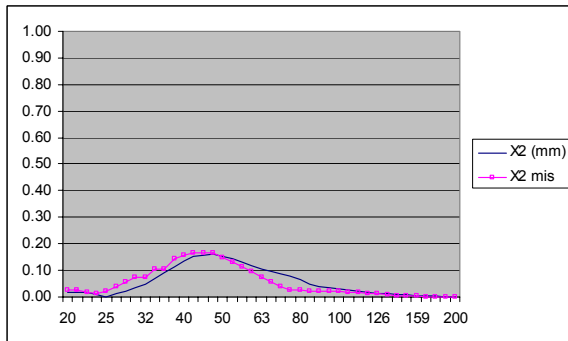


Fig. 6.3. Sample #05: 2nd harmonic curve of moving mass excursion. Loudspeaker driven @ 6V. (\*)

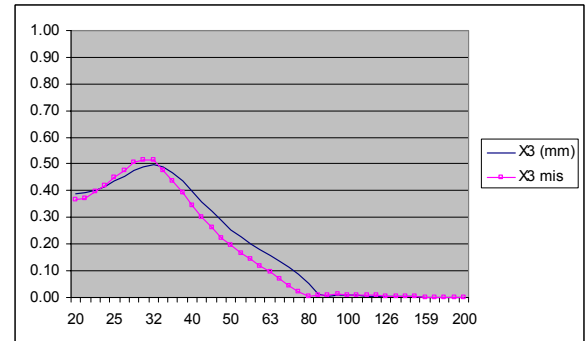


Fig. 6.4 Sample #05: 3rd harmonic curve of moving mass excursion. Loudspeaker driven @ 6V. (\*)

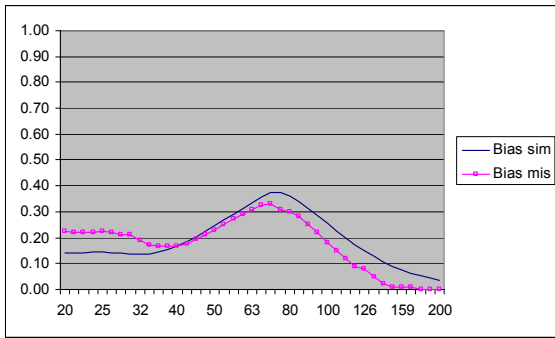


Fig. 7.1. Sample #05: bias curve associated to the moving mass equilibrium point. Loudspeaker driven @4V. (\*)

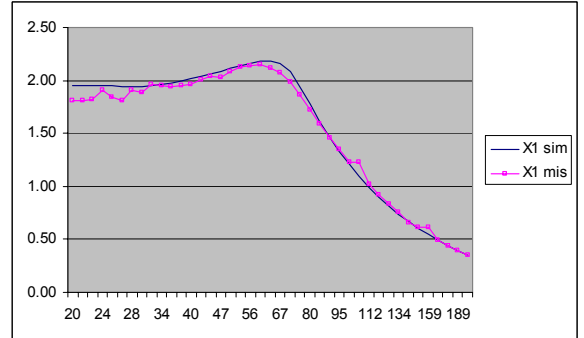


Fig. 7.2. Sample #05: 1st harmonic curve (fundamental) of moving mass excursion. Loudspeaker driven @ 4V. (\*)

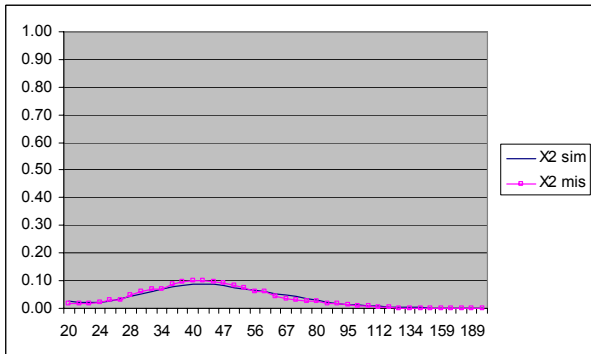


Fig. 7.3. Sample #05: 2nd harmonic curve of moving mass excursion. Loudspeaker driven @ 4V. (\*)

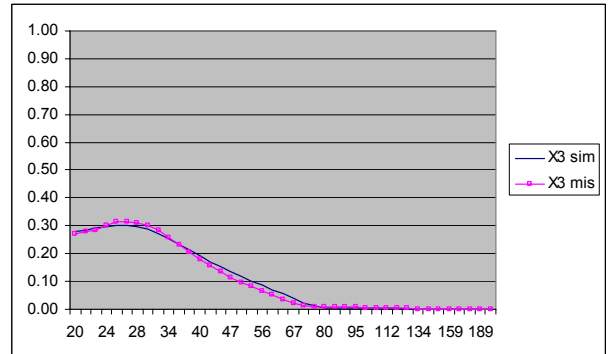


Fig. 7.4. Sample #05: 3rd harmonic curve of moving mass excursion. Loudspeaker driven @ 4V (\*)

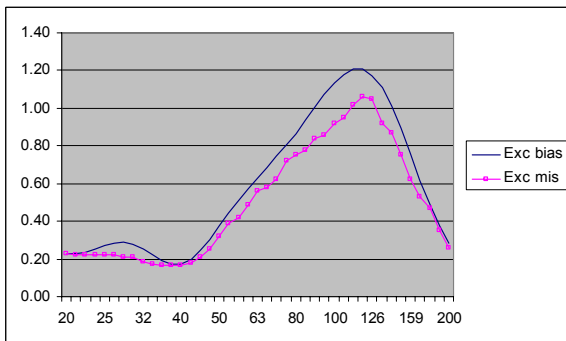


Fig. 8.1. Sample #05: bias curve associated to the moving mass equilibrium point. Loudspeaker driven @6V. (\*\*)

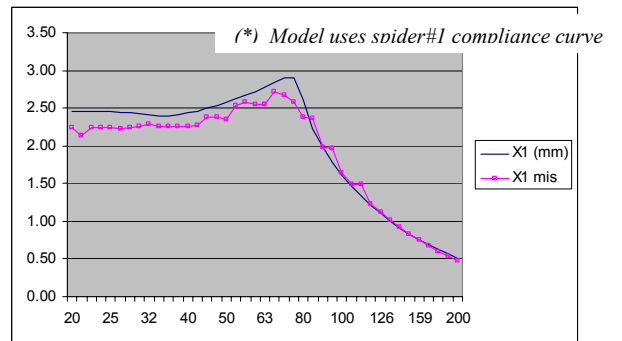


Fig. 8.2. Sample #05: 1st (fundamental) harmonic curve of moving mass excursion. Loudspeaker driven @ 6V. (\*\*)

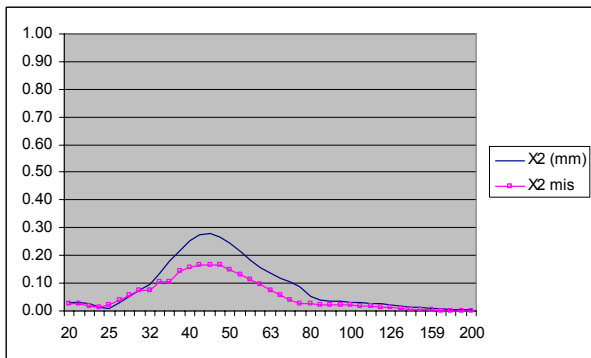


Fig. 8.3. Sample #05: 2nd harmonic curve of moving mass excursion. Loudspeaker driven @ 6V. (\*\*)

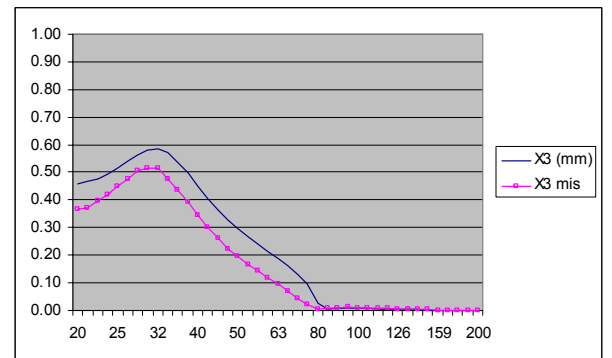


Fig. 8.4. Sample #05: 3rd harmonic curve of moving mass excursion. Loudspeaker driven @ 6V. (\*\*)

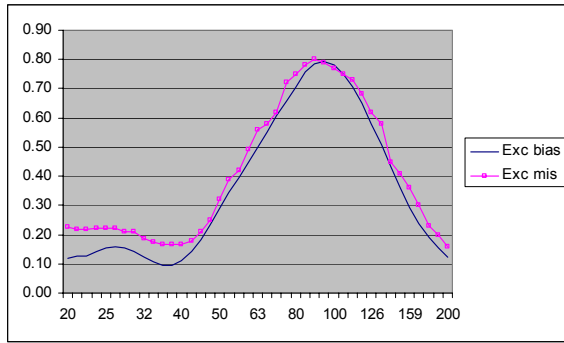


Fig. 9.1. Sample #03: bias curve associated to the moving mass equilibrium point. Loudspeaker driven @6V.

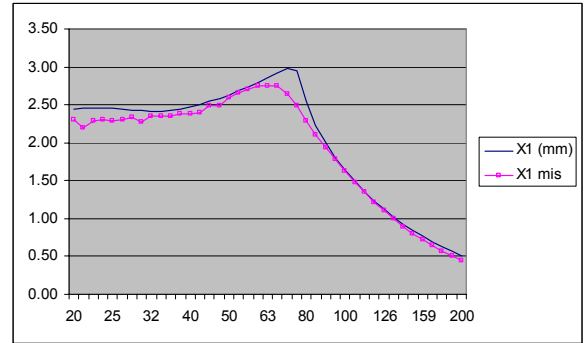


Fig. 9.2. Sample #03: 1st (fundamental) harmonic curve of moving mass excursion. Loudspeaker driven @ 6V.

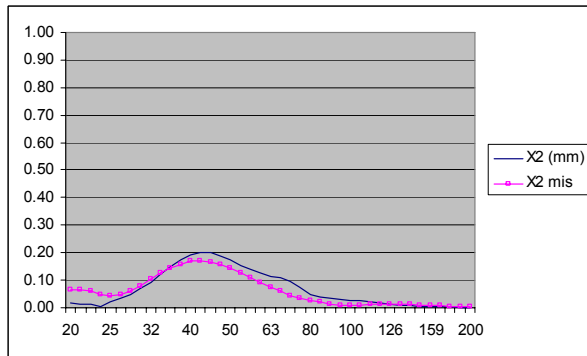


Fig. 9.3. Sample #03: 2nd harmonic curve of moving mass excursion. Loudspeaker driven @ 6V.

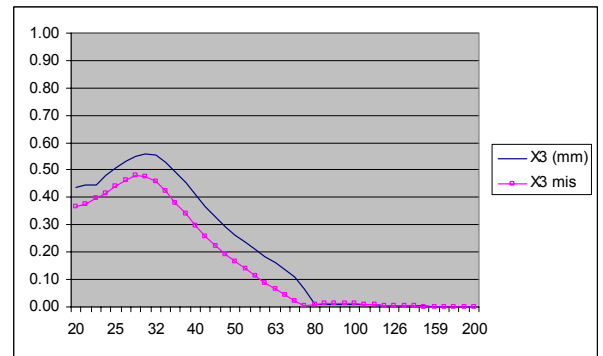


Fig. 9.4 Sample #03: 3rd harmonic curve of moving mass excursion. Loudspeaker driven @ 6V.

(\*\*) Model uses spider# 2 compliance curve

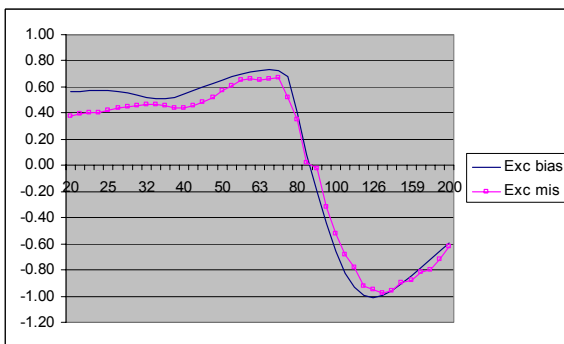


Fig. 10.1. Sample #12 (voice coil on-field position offset = -1.0mm): Bias curve associated to the moving mass equilibrium point. Loudspeaker driven @6V.

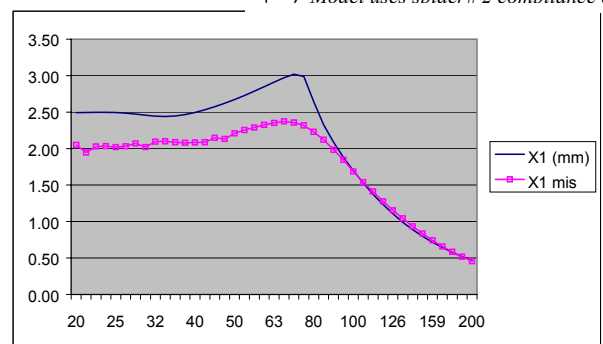


Fig. 10.2. Sample #12 (voice coil on-field position offset = -1.0mm): 1st (fundamental) harmonic curve of moving mass excursion. Loudspeaker driven @ 6V.

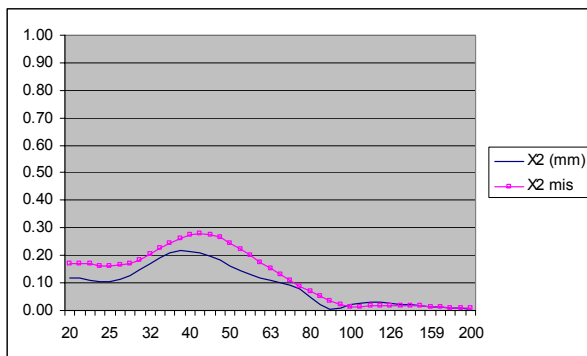


Fig. 10.3 Sample #12 (voice coil on-field position offset = -1.0mm): 2nd harmonic curve of moving mass excursion. Loudspeaker driven @ 6V.

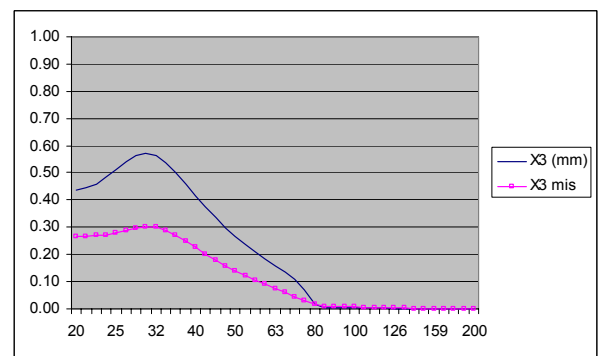


Fig. 10.4. Sample #12 (voice coil on-field position offset = -1.0mm): 3rd harmonic curve of moving mass excursion. Loudspeaker driven @ 6V.

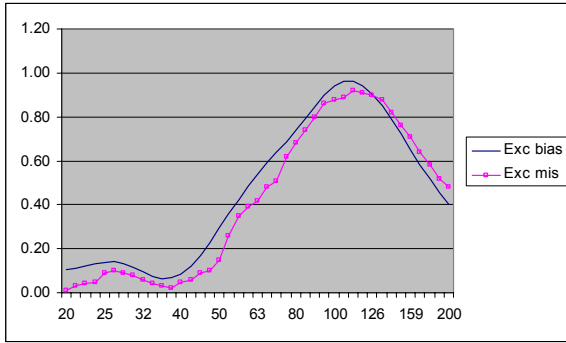


Fig. 11.1. Sample #13 (augmented voice coil height: +2.0mm): bias curve associated to the moving mass equilibrium point. Loudspeaker driven @6V.

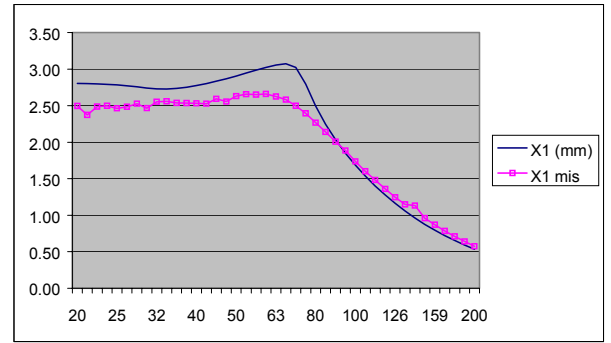


Fig. 11.2 Sample #13 (augmented voice coil height: +2.0mm): 1<sup>st</sup> (fundamental) harmonic curve of moving mass excursion. Loudspeaker driven @ 6V.

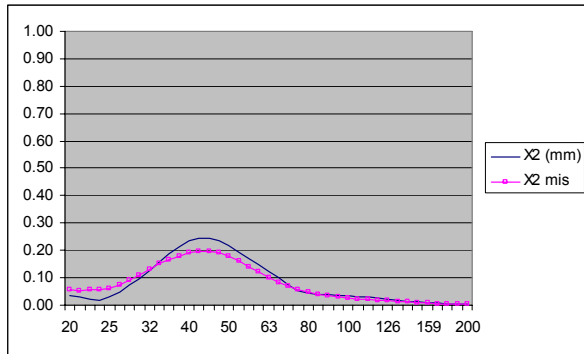


Fig. 11.3. Sample #13 (augmented voice coil height: +2.0mm): 2nd harmonic curve of moving mass excursion. Loudspeaker driven @ 6V

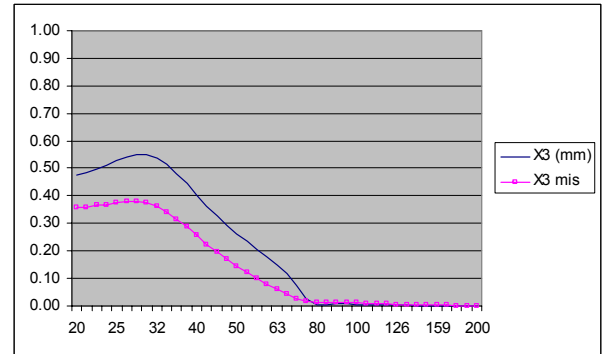


Fig. 11.4. Sample #13 (augmented voice coil height: +2.0mm): 3<sup>rd</sup> harmonic curve of moving mass excursion. Loudspeaker driven @ 6V

---

## References

---

- [1] R.H. Small, “Direct-Radiator Loudspeaker System Analysis”, in Loudspeakers vol. 1 (Audio Engineering Society, New York, 1978)
- [2] R.H. Small, “Closed-Box Loudspeaker System, Part I: Analysis ”, in Loudspeakers vol. 1 (Audio Engineering Society, New York, 1978)
- [3] A. N. Thiele, “Loudspeakers in Vented Boxes: Part I and II”, in Loudspeakers vol. 1 (Audio Engineering Society, New York, 1978)
- [4] W. Klippel, “Measurement of Large-Signal Parameters of Electrodynamical Transducer”, Presented to the 107th convention of the Audio Eng. Soc., Sept. 1999, Preprint 5008.
- [5] W. Klippel, “Fast and Accurate Measurement of Linear Transducer Parameters ”, Presented to the 110th convention of the Audio Eng. Soc., May 2001, Preprint 5308
- [6] D. Clark and R.J. Mihelich, “Modelling and Controlling Excursion-Related Distortion in Loudspeakers”, Presented to the 106th convention of the Audio Eng. Soc., May 1999, Preprint 4862
- [7] D. Clark, “Precision Measurement of Loudspeakers Parameters”, *J Audio Eng. Soc.*, vol. 45, pp. 129-141 (Mar. 1997)
- [8] T. Heed, “Quantitative Analysis of Low Frequency Component Nonlinearities”, Presented to the 101th convention of the Audio Eng. Soc., Nov. 1996, Preprint 4332
- [9] D. Clark, “Blat Distortion in Loudspeakers ”, Presented to the SAE Congress, Feb. 1995, Preprint 950189